

Quantifying the inter- and intra-granular stresses and their effects on deformation behaviors for the polycrystalline hexagonal beryllium by neutron diffraction



Changsheng Zhang*, Hongjia Li, Beibei Pang, Hong Wang, Jian Li, Zukun Yang, Guangai Sun*

Key Laboratory for Neutron Physics of Chinese Academy of Engineering Physics, Institute of Nuclear Physics and Chemistry, Mianyang 621999, China

ARTICLE INFO

Keywords:

Hexagonal metals
Multiscale internal stresses
Neutron diffraction
Deformation mechanism
Temperature and strain rate effects

ABSTRACT

The internal stresses developing at different length scales play the important role in materials performance. This importance has been well recognized for the cubic metals, however, not for the hexagonal close-packed (hcp) ones. The present work investigates the intergranular and intragranular stresses in the polycrystalline hexagonal beryllium by neutron diffraction. The correlation between those internal stresses and the deformation mechanism is revealed, and the strain rate and temperature effects on those stresses are presented. A composite behavior of intergranular and intragranular stresses is observed, which can be significantly tuned by the temperature and strain rate effects. The intergranular stress and stored energy are large for the soft-oriented grains (SOGs), while the intragranular stress and stored energy are large for the hard-oriented ones (HOGs). Both of those stresses are significantly high for the dynamic strain rate while they are relatively low for the elevated temperature. The large internal stresses in the dynamically compressed specimen should be attributed to the large number of twins and high density of dislocations. Different HOGs-SOGs configurations are proposed on the light of those observations, which might facilitate the properties controlling and extend the application scope for the hcp metal beryllium.

1. Introduction

The hexagonal close-packed (hcp) metal beryllium and other ones (such as titanium and magnesium) have attracted much attention due to both the intense scientific interest and significant technological importance [1–5]. However, the hcp structure brings greatly the complication in the deformation mechanisms [1–3], which poses the significant challenges in the science advancement and engineering development for hcp metals. Pronounced efforts have been therefore deployed to understand the deformation mechanisms in hcp metals, which include the dislocation slip [2,3,6,7], twinning [1,8–10], and the interaction between the slip and twinning [1,11,12].

The deformation process is also accompanied with the internal stresses, which develop at different length scales from the subgrain to the complete structure [13,14]. These stresses can result in the damage and failure (e.g., plastic collapse and fatigue) by the interaction with other microstructural influences [15–17]. For the metals with the simpler cubic structure, the importance of those multiscale internal stresses has been well recognized, which have been deemed as the fingerprints for the deformation and damage [18–20].

However, only limited data on those internal stresses are available for the hcp metals despite the numerous efforts on understanding the deformation mechanisms. For instance, only the uniaxial lattice strain along the loading axis has been intensively observed as a function of the applied stress [21–24], which can be utilized to understand the mechanical response in the microscopic scale. While a reasonable knowledge base is built for such microstress evolution during deformation, little is nevertheless known about the distribution of the multiscale internal stresses in the hcp metals. Consequently, some questions are still open, including the grain-orientation dependence of those internal stresses, and the correlation between those stresses and the deformation mechanisms. Furthermore, from the application point of view, the effects of strain rate and temperature on mechanical performances are of technological importance [25,26]. For instance, when used as the first wall armoring material in fusion reactors, beryllium would bear the extremely high pressures and temperatures [27,28]. Therefore, it is significantly essential to clarify the effects of temperature (T) and strain rate ($\dot{\epsilon}$) on the multiscale internal stresses in this hcp metal.

The objective of the present paper is to provide the experimental data on the multiscale (intragranular and intergranular) stresses for

* Corresponding authors.

E-mail addresses: inpc_zhang@163.com (C. Zhang), guangaisun_80@163.com (G. Sun).

<https://doi.org/10.1016/j.matchar.2018.09.014>

Received 16 May 2018; Received in revised form 8 September 2018; Accepted 10 September 2018

Available online 15 September 2018

1044-5803/ © 2018 Elsevier Inc. All rights reserved.

Table 1
The nominal composition (in wt%) of the HP beryllium.

Be (\geq wt%)	Impurities (\leq wt%)							
	Fe	Al	Si	Ti	Cr	O	C	Others
99	0.15	0.013	0.021	0.021	0.029	0.65	0.05	0.062

beryllium, which are necessary to improve the understanding of deformation mechanism. A composite behavior of intergranular and intragranular stresses in polycrystalline beryllium is revealed, which can be tuned by the temperature and strain rate effects. On the light of these observations, some insights are further brought into the properties controlling and materials design for hcp metals.

2. Materials and Experiments

The hot-pressed (HP) beryllium materials were provided by Northwest Rare Metal Materials Research Institute (NRMRI), with the nominal composition as listed in Table 1. The specimens were machined into the rods with 5 mm in diameter and 5 mm in height. The height direction was along the axis of HP beryllium ingots. The quasi-static (for $10^{-3} \text{ s}^{-1} \leq \dot{\epsilon} \leq 10^{-1} \text{ s}^{-1}$) and dynamic (for $\dot{\epsilon} \geq 10^3 \text{ s}^{-1}$) compression tests were performed on a hydraulic load frame and Split-Hopkinson Pressure Bar (SHPB), respectively. Those specimens were continuously compressed up to 20% strain, where the compressive stress was then interrupted and unloaded. The stress loading direction (LD) is parallel to the height direction. Several pole figures (PFs), including (10.0), (00.2), (10.1), (10.2), (11.0), and (10.3) PFs, were measured for the as-received (i.e., uncompressed) and compressed specimens on Residual Stress Neutron Diffractometer (RSND) at China Mianyang Research Reactor (CMRR) [29]. These compressed specimens were the one compressed respectively (i) at $\dot{\epsilon} = 10^{-3} \text{ s}^{-1}$ and room temperature (RT), (ii) at $\dot{\epsilon} = 10^{-3} \text{ s}^{-1}$ and the elevated temperature (e.g., $T = 600 \text{ }^\circ\text{C}$), and (iii) at $\dot{\epsilon} = 2500 \text{ s}^{-1}$ and RT. Each PF was measured by utilizing the Kappa goniometer, as schematically illustrated in Fig. 1(a). The specimen coordinate was defined by the three-dimensional (3D) directions, namely the loading direction (LD), radial direction (RD) and transverse direction (TD). Note that RD is equivalent to TD according to the transversal isotropy associated with the specimen shape. The measurement of different PFs was carried out by

altering the diffraction angle ($2\theta_{hk.l}$). The diffraction patterns were simultaneously collected when the tilting and rotation angles (denoted respectively as ψ and χ) were continuously increased up to 90° and 360° , respectively. The in-situ neutron diffraction measurements were also carried out on RSND. The cylindrical specimen, with 5 mm in diameter and 10 mm in length, was quasistatically compressed at RT and 10^{-3} s^{-1} through the stress loading cell, which was installed in the center of sample table of RSND. The macroscopic and microscopic strains in the orientation $\langle hk.l \rangle$ parallel to the loading direction (LD) were simultaneously measured during compression. The experimental setup of in-situ neutron diffraction is shown in Fig. 1(b). During the measurement, the $(hk.l)$ reflection was selected through adjusting the diffraction angle ($2\theta_{hk.l}$). During each scanning for the $(hk.l)$ reflection, the scattering vector (q) was always parallel to the LD (also the height direction) of the sample through the rotation of sample table. The wavelength (λ) of 1.587 \AA was employed for both the PFs and in-situ measurements. All the two-dimensional diffraction patterns collected during the PFs and in-situ measurements were analyzed by using the *StressTextureCalculator (STeCa)* software [30]. Through this procedure, the profile-related data, including the peak position, width and intensity, were simultaneously obtained. The lattice strains ($\epsilon_{hk.l}$) were then calculated by the following equation:

$$\epsilon_{hk.l} = (d_{hk.l} - d_{hk.l,0})/d_{hk.l,0} = (\sin \theta_{hk.l,0}/\sin \theta_{hk.l}) - 1, \quad (1)$$

where $d_{hk.l}$ and $\theta_{hk.l}$ denote the lattice spacing for the $(hk.l)$ plane and peak position, respectively, with $d_{hk.l,0}$ and $\theta_{hk.l,0}$ being the corresponding values for the stress-free condition. All the peak profiles for the measurement points (ψ, χ) were carefully analyzed to acquire the intragranular and intergranular strains as well as the distribution for them. Multiple PFs data were used to the orientation distribution function (ODF) analysis, which was carried out through the *MTEX* package [31].

3. Results

3.1. Macroscopic Mechanical Behaviors

Fig. 2(a) shows the macroscopic mechanical behavior of HP beryllium, which is strongly dependent on the temperature (T) and strain rate ($\dot{\epsilon}$). It is obviously observed that the high strain rate induces the hardening while the elevated temperature induces the softening in the mechanical behavior. At room temperature (RT), the applied

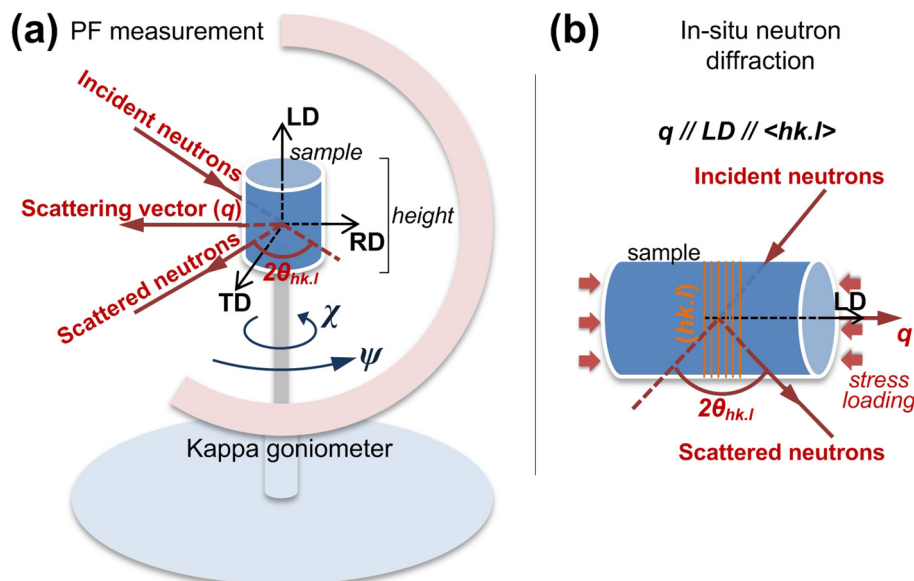


Fig. 1. Schematic illustration of the experimental setups for PF measurement (a) and in-situ neutron diffraction (b), respectively.

Download English Version:

<https://daneshyari.com/en/article/10128688>

Download Persian Version:

<https://daneshyari.com/article/10128688>

[Daneshyari.com](https://daneshyari.com)